

Numerical Modelling and Comparison with Experiments on MARFEs in TEXTOR-94

D.Reiser¹, R.Zagórski², H.Gerhauser¹, J.Rapp¹, H.A.Claaßen¹,
M.Z.Tokar¹, P.Börner¹, B.Küppers¹

¹*Institut für Plasmaphysik, Forschungszentrum Jülich GmbH,
EURATOM Association, Trilateral Euregio Cluster, D-52425 Jülich, GERMANY.*

²*Institute of Plasma Physics and Laser Microfusion, P.O.Box 49, 00-908 Warsaw, POLAND.*

1 Introduction

The 2D edge codes TECXY [1,2] and B2-EIRENE [3,4] have been proved to be useful tools for investigating specific physical questions in the plasma edge of limiter tokamaks.

In the present paper we apply both codes to study the evolution of the so-called MARFEs, thermal instabilities which arise locally in a zone near the high-field side of the TEXTOR boundary layer [5,6], as a result of strong plasma cooling by the interaction with the deuterons recycled at the bumper limiter, and by the subsequent highly increased radiation which is limited by the heat transport along the magnetic field and radially from the core.

2 Physical Model

The 2D edge codes TECXY [1,2] and B2 [3] are primarily based on the classical transport equations derived by Braginskij [7]. The model describes the electrons and various ion species in their different charge states as separate fluids. The transport along field lines is assumed to be classical and transport coefficients follow from the 21-moment Grad approximation [9,10]. The radial transport is assumed to be anomalous with prescribed radial transport coefficients of the order of Bohm diffusion and Alcator-like radial dependence. All ion species have the same temperature T_i , which can be different from the electron temperature T_e . Equations of different fluids are coupled by electrostatic, friction and thermal forces as well as by atomic processes such as collisional ionization, recombination (dielectronic and radiative), excitation and charge exchange. Besides these common features the different codes include refinements of the physical model in different directions: In order to consider drift motions and currents in the tokamak boundary layer, additional equations were added in the TECXY-code, which have been obtained from the radial and diamagnetic components of Ohm's law and the equation of motion [1,2].

In the B2-EIRENE-calculations the drift motions and currents were neglected, but the analytical neutral model of the TECXY-code is replaced by a detailed description of the neutral transport on the basis of a kinetic model [4].

In the TECXY-calculations standard boundary conditions were used [1,2,8]. At the core boundary input particle Γ_{inp} and energy fluxes Q_{inp} have been prescribed. For impurity ions we have assumed a zero total carbon ion flux across the core boundary [8]. At the wall we have used decay lengths as boundary conditions for the densities and temperatures (with $\lambda = 2 \text{ cm}$) [1,2]. The standard sheath boundary conditions are used for the parallel transport at the limiter plates [11]. The dynamics of deuterium and impurity neutrals in the neighbourhood of the ALT-II limiter is described by an analytical model [8], which accounts in a selfconsistent way for recycling of plasma ions as well as for sputtering processes at the limiter plates. Only physical sputtering

by deuterium ions and self-sputtering of carbon atoms are considered in the model. In order to model the bumper limiter (BL) we have assumed high additional recombination losses inside this region and a suitably chosen profile for the recycled neutrals penetrating from the bumper surface into the adjacent plasma (see Fig.1). For impurity atoms a similar model has been used. In the case of carbon atoms we have assumed that apart from impurity atoms recycling at the

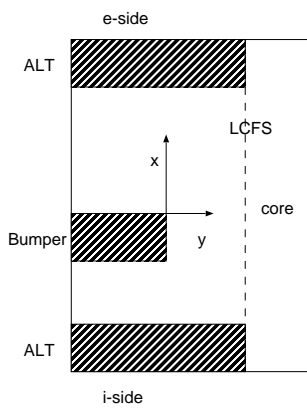


Fig. 1: Sketch of the calculational region of TEXTOR-94.

BL we have an additional influx Γ_{bump}^C of impurity atoms from the BL due to sputtering processes. We have taken Γ_{bump}^C equal to 2.5 % of the plasma flux to the BL.

In the B2-EIRENE-calculations we used also standard sheath boundary conditions for the parallel transport and a kind of decay length model for the radial transport [12] at the limiter surfaces. As mentioned above the neutral distribution is not prescribed, but selfconsistently calculated. In contrast to the TECXY-calculations the energy influx and the density were fixed at the core boundary. For the radial transport coefficients we used constant values for simplicity, chosen in a similar range as for TECXY. The calculations were performed on a radially larger grid covering the plasma region $0.3 \text{ m} \leq r \leq 0.5 \text{ m}$ which allows to do a line-of-sight-analysis of the resulting carbon radiation for comparison with experimental results.

3 Results and Conclusions

TECXY-calculations have been performed for a high density auxiliary heated TEXTOR discharge in deuterium with carbon as the dominant intrinsic impurity element. The belt limiter

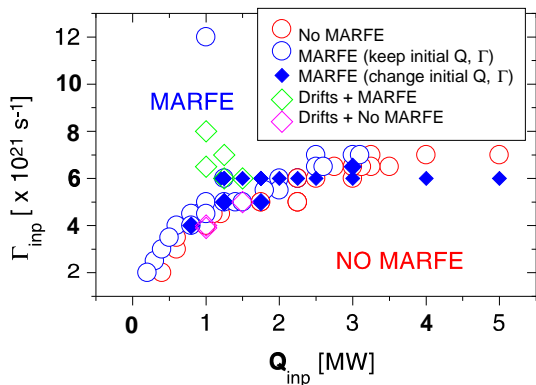


Fig. 2: Stability diagram: particle influx vs input power.

ALT-II is at $\theta = -45^\circ$ position, the total magnetic field $B = 2.25 \text{ T}$ and the Shafranov shift $\Delta = 6 \text{ cm}$. The anomalous transport in radial direction is determined by the coefficients $D_{\perp}^a(y) = 0.6 (1 + (y/y_s)^2) \text{ m}^2/\text{s}$, where $y_s = 4 \text{ cm}$ is the position of the separatrix, and $\eta_{\perp}^a = \frac{1}{3} D_{\perp}^a$, $\chi_{\perp}^e/n_e = \frac{3}{2} \chi_{\perp}^a/n_a = 2 D_{\perp}^a$ assuming a limit of $D_{\perp}^a = 1.2 \text{ m}^2/\text{s}$ for $y > y_s$. The bumper limiter is introduced into the scrape-off layer in a region between -45° and $+45^\circ$ below and above the high-field side, leaving a width of about 2 cm between the bumper surface and the last closed flux surface. The calculations were performed assuming a recycling of 75 %. First we have made a series of calculations for a deuterium plasma (without impurities) varying the input particle and energy fluxes: $2 \times 10^{21} \text{ s}^{-1} < \Gamma_{inp} < 1.2 \times 10^{22} \text{ s}^{-1}$ and $0.2 \text{ MW} < Q_{inp} < 5 \text{ MW}$, respectively. This parameter study shows that for sufficiently high particle influx into (density level in) the plasma edge layer and/or sufficiently low energy influx (temperature level) a stability boundary is crossed and the MARFE develops (Fig.2). The stability boundary between the MARFE and the no-MARFE region is not sharp because bifurcated solutions are possible which depend on the history (initial conditions) of the plasma. Critical values (taken at the separatrix and the low-field side) which always produce MARFEs are densities $n_e \gtrsim 8 \times 10^{18}/\text{m}^3$ or temperatures $(T_e + T_i)/2 \lesssim 50 \text{ eV}$. Within the MARFE n_e increases up to $10^{20}/\text{m}^3$ and T_e, T_i decrease

down to 4 eV. The effect of drifts as found by TECXY is a shift of the MARFE position towards the upper bumper edge and a weakening of the MARFE strength, but the stability boundary seems to be not affected. Time dependent calculations of the MARFE evolution showed that the typical time of MARFE development is of the order of 1–2 ms in the case without impurities. In Fig.3 a comparison of the MARFE onset between experimental and calculated results is shown. It can be seen that the experimentally found scaling relations are very well reproduced by the

TECXY results. The threshold plasma density is higher in calculations than in the experiment since the influence of impurities has been neglected. Also the T_e increase with power input is too steep in the absence of impurities which tend to stabilize the edge T_e near 50 eV. If impurities are considered in the calculations then the MARFE appears at a lower density $n_e \lesssim 6.2 \times 10^{18}/\text{m}^3$ because of the additional cooling due to radiation from impurity ions. The time evolution of the plasma parameters at the MARFE position for the case with impurities is now on a much longer time scale of the order of 5 ms without drifts and 10 ms with drifts.

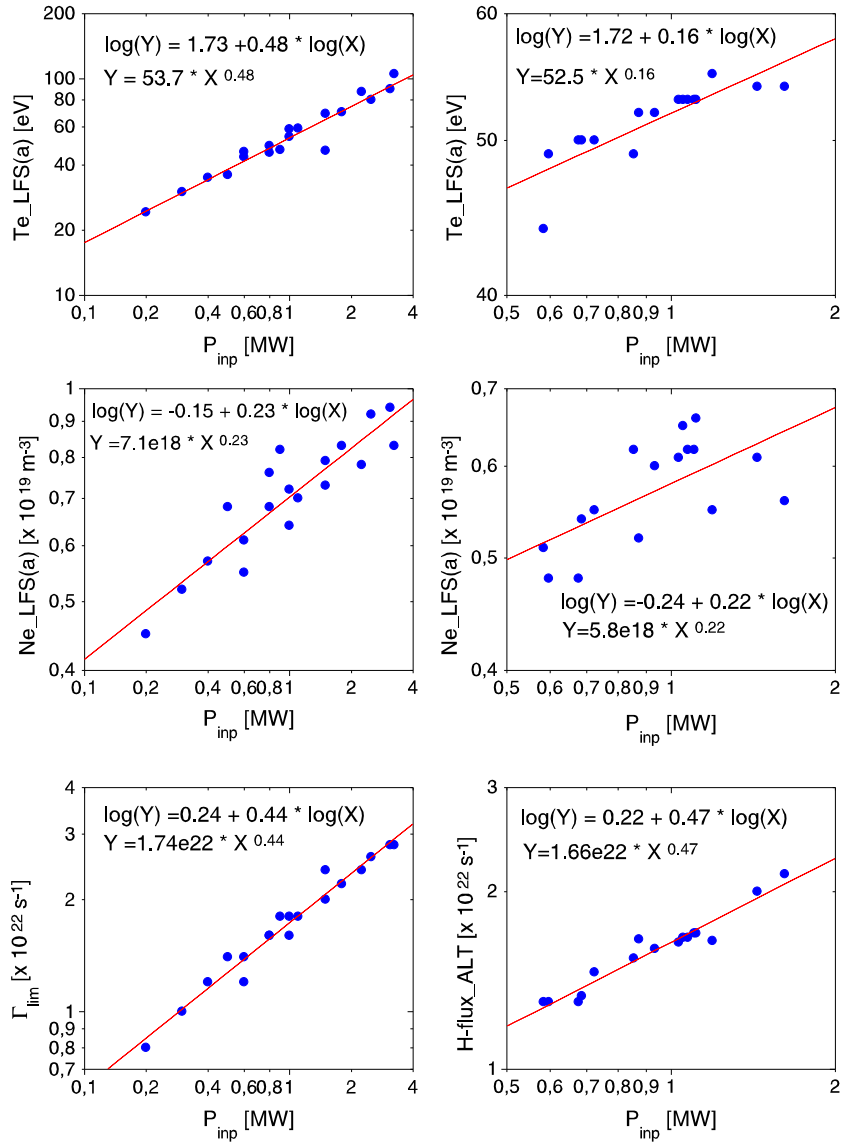


Fig. 3: MARFE onset: calculated (left) and experimentally [13] observed (right) scaling laws.

The B2-EIRENE-calculations were performed for both, pure hydrogen plasmas and hydrogen-carbon-plasmas. In the studies we focussed on stationary states of MARFE-like plasmas and did not analyse the time evolution. As in the TECXY results we observed MARFEs for pure hydrogen plasmas and plasmas with impurities as well. The calculations were done for several fixed densities at the core boundary and confirm the results above, i.e. a rise of the densities and a lowering of the temperatures in the MARFEs for the cases with additional cooling due to carbon radiation. The line-of-sight-analysis of selected carbon lines showed good agreement with ex-

perimental results of the UV-spectroscopy, but in the calculations with a constant $D_{\perp} = 2 \text{ m}^2/\text{s}$ the average electron density was by a factor of 2 above the experimentally observed densities. This could be removed by the use of $D_{\perp} = 1 \text{ m}^2/\text{s}$ again in agreement with the TECXY-results. Besides lowering the temperature in the MARFE, the carbon impurities have also the effect that the impurity cloud can spread out much more into the plasma, and as a result the MARFE will be swept towards the i-side of the ALT-II limiter by the flow field of the background plasma. This may be one explanation of the experimentally observed downward shift of the MARFEs. Fig.4 shows the plasma flow patterns for two different bumper positions, which result from the

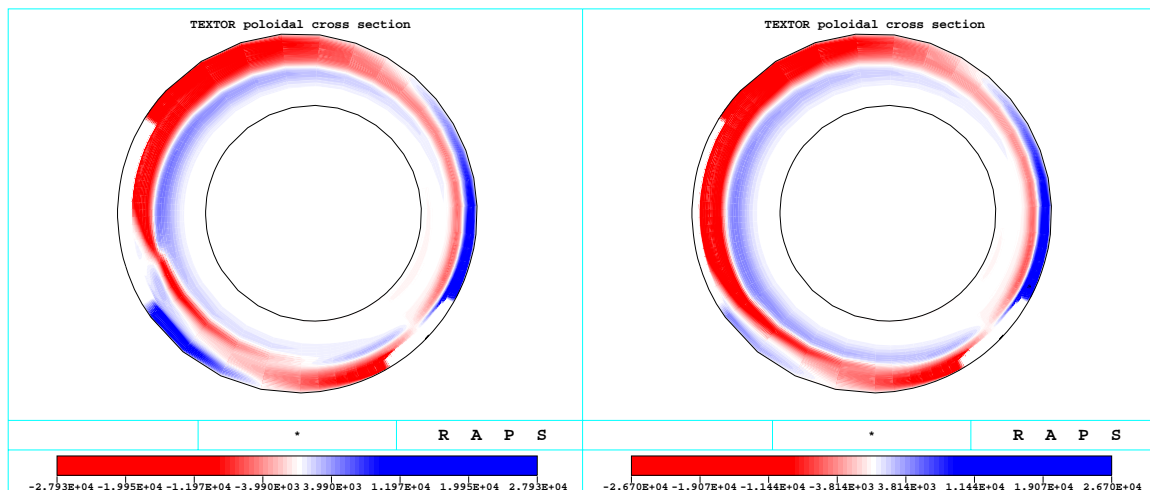


Fig. 4: Flow patterns for different bumper positions. (a) 1.0 cm and (b) 2.5 cm distance from separatrix. Blue marks the clockwise direction and red the counter-clockwise direction. The (parallel) velocities are given in m/s.

asymmetrically located ALT-II. For a distance of about 1 cm between the bumper surface and the separatrix a very pronounced flow at the bumper directed towards the ALT-II can be seen. For a larger distance of the bumper this directed flow is even more pronounced, and the MARFE will be moved much farther towards the ALT-II, as observed in experiments for different plasma positions.

4 References

- [1] R.Zagórski, H.Gerhauser, H.A.Claaßen, Contrib. Plasma Physics **38** (1998) 61
- [2] R.Zagórski, H.Gerhauser, H.A.Claaßen, J. Nucl.Mat., **266-269** (1999) 1261
- [3] Braams, B.J., Net-Rep. EUR-FU IXII-80-87-68, Comm. of the Europ. Communities (1987)
- [4] Reiter, D., J. Nucl.Mat. **196-198**, p.80 (1992)
- [5] U. Samm et al., J.Nucl.Mat. **266-269** (1999) 666
- [6] M.Z. Tokar' et al., J.Nucl.Mat. **266-269** (1999) 958
- [7] S.I. Braginskij, Rev. Plasma Phys. **1** (1965) 205
- [8] R.Zagórski, J.Techn.Phys. **37(1)** (1996) 7
- [9] Yu.L. Igitkhanov et al., Proc. 14th EPS Conf. on CFPP, Madrid (1987), Pt.II, p.760
- [10] H.A. Claaßen, H.Gerhauser, R.N.El-Sharif, Report of KFA Jülich, **JÜL-2423** (Jan.1991)
- [11] H.Gerhauser, H.A.Claaßen, J.Nucl.Mat. **176&177** (1990) 721
- [12] P.C.Stangeby et al.,Nucl.Fusion, Vol.32, No.12 (1992)
- [13] J.Rapp et al., this conference